Intracranial Injectable Tumor Model: Technical Advancements

Cristian Gragnaniello[1] Filippo Gagliardi[2] Anthony M.T. Chau[1] Remi Nader[3] Alan Siu[4] Zachary Litvack[4] Bruno De Luca[5] Kevin Seex[1] Pietro Mortini[2] Anthony J. Caputy[4] Ossama Al-Mefty[6]

[1] Macquarie Neurosurgery, Australian School of Advanced Medicine, Macquarie University, Sydney, Australia
[2] Department of Neurosurgery, Vita-Salute University, San Raffaele Scientific Institute, Milan, Italy
[3] Department of Neurosurgery, Texas Center for Neurosciences, Beaumont, Texas, United States
[4] Department of Neurosurgery, George Washington University, Washington District of Columbia, United States
[5] Department of Experimental Medicine, Second University of Naples, Naples, Italy
[6] Department of Neurosurgery, Brigham and Women's Hospital, Boston, Massachusetts, United States

Address for correspondence Cristian Gragnaniello, MD, PhD, MSurg, MAdvSurg, Suite 2, Level 2, 2 Technology Place, Macquarie University, NSW 2109, Sydney, Australia (e-mail: cristian.neuro@gmail.com; cristian@mqneurosurgery.com).

J Neurol Surg B 2014;75:301–308.

Abstract

Background and Objectives Few simulation models are available that provide neurosurgical trainees with the challenge of distorted skull base anatomy despite increasing importance in the acquisition of safe microsurgical and endoscopic techniques. We have previously reported a unique training model for skull base neurosurgery where a polymer is injected into a cadaveric head where it solidifies to mimic a skull base tumor for resection. This model, however, required injection of the polymer under direct surgical vision via a complicated alternative approach to that being studied, prohibiting its uptake in many neurosurgical laboratories.

Conclusion We report our updated skull base tumor model that is contrast-enhanced and may be easily and reliably injected under fluoroscopic guidance. We have identified a map of burr holes and injection corridors available to place tumor at various intracranial sites. Additionally, the updated tumor model allows for the creation of mass effect, and we detail the variation of polymer preparation to mimic different tumor properties. These advancements will increase the practicality of the tumor model and ideally influence neurosurgical standards of training.

Keywords
- neurosurgical training
- skull base
- tumor model
- microsurgery

Introduction

Skull base neurosurgery has benefited enormously from the technical advancements of modern microsurgery and endoscopic surgery. With these developments have come increasing demands for laboratory training models to prepare new generations of neurosurgeons for the complicated and demanding narrow corridor pathologic anatomy of space-occupying skull base lesions. We have previously reported a unique training model for skull base neurosurgery where a polymer is injected into a cadaveric head to mimic a skull base tumor for resection.[1] This model, however, required injection of the polymer under direct surgical vision via a complicated alternative approach to that being studied, followed by expensive magnetic resonance imaging (MRI) or computed tomography (CT) to localize the lesion and plan the skull base

received
October 5, 2013
accepted after revision
November 22, 2013
published online
July 21, 2014

DOI http://dx.doi.org/10.1055/s-0034-1368148.
ISSN 2193-6331.

surgical approach. We recognized that these two major drawbacks may be prohibitive in many neurosurgical laboratories, and so we have addressed this in our substantially modified and simplified tumor model, which we report here.

Material and Methods

Cadaveric Heads Preparation

Six cadaveric head specimens were prepared using standard formaldehyde fixation and injected colored latex techniques, as described previously by Sanan et al.[2]

Tumor Preparation

As described previously by our group,[1] Stratathane resin ST-504 (SRS, Strata-Tech Inc.) is a polymer that when it solidifies closely resembles the physical characteristics of extra-axial tumors. The polymer is a solvent-free, water-based, initially nonviscous liquid that can be injected into the skull base, where it spreads through subarachnoid routes to encase neurovascular structures. One to 4 minutes after injection, it foams into a highly stable, hydrophobic, solid gel that encases and gently displaces anatomical structures without adhering to them. Various solvents have been tested to improve the adhesiveness, texture, subarachnoid spread potential, deformability, and radiologic visibility of SRS.

These investigations have led to the development of a novel compound that we named Stratathane resin ST-504 derived polymer (SRSDP), which mimics intra- and extra-axial cranial tumors for use in neurosurgical training both in the skull base and cerebral/ventricular system. The SRSDP is a water-based, iodide contrast-enhanced substance that similarly cures to become a gel and demonstrates the same spreading and coagulating capacity. The polymer matrix is visible on skull X-rays and CT as a strongly contrast-enhancing substance. A variant of SRSDP was also developed to simulate calcified lesions such as meningiomas and oligoastrocytomas, which we termed calcified SRSDP (cSRSDP). This contained fine sand or small bone fragments taken from the burr hole.

An experiment was designed to mix nine different ratios of SRSDP with water. SRSDP was distributed, 1 mL each, into nine plastic cups. Water was added into the cups to form a mixture with a volume ratio of 1:10 (one portion of SRSDP to 10 portion of water) and 1:9, 1:8, 1:7, 1:6, 1:5, 1:4, 1:3, and 1:2, respectively. Each mixture was blended and stirred until it started to foam. ►**Table 1** reports the physical and chemical characteristics of SRSDP as well as polymerization time at varying polymer concentrations.

Table 1 Polymerization times and characteristics of ST-504 derived polymer at varying polymer concentrations

	Polymerization	Deformability	Viscosity	Adhesiveness	Gumminess	Friability	Stringing
1:10	2′ 10″	+	+	+	+ + + + + +	+	+
1:9	2′ 10″	+	+ +	+	+ + + + +	+ +	+
1:8	2′ 10″	+ +	+ +	+ +	+ + + +	+ +	+ +
1:7	1′ 55″	+ +	+ +	+ +	+ + +	+ +	+ +
1:6	1′ 55″	+ +	+ +	+ +	+ +	+ +	+ +
1:5	1′ 54″	+ +	+ +	+ +	+	+ +	+ +
1:4	1′ 54″	+ +	+ +	+ +	+	+ +	+ +
1:3	1′ 53″	+ +	+ +	+ +	+	+ +	+ +
1:2	1′ 52″	+ +	+ +	+ +	+	+ +	+ +

Tumor Injection Technique

Recognition of Shortcomings and Need for Simplification

We recognized that the process of tumor placement under direct vision requires complicated and time-consuming surgical approaches, such as a transoral injection route for a far-lateral transcondylar resection or an endonasal injection route for a retrosigmoid cerebellopontine angle (CPA) resection. Another significant problem was that in vitro, the polymer had the capacity to foam up to five times its initial

Table 2 Burr holes and injection corridors map

Burr hole site	Anatomical corridor	Lesion site	Surgical corridor
Nasion	Subfrontal Interhemispheric	Olfactory groove Planum sphenoidale Anterior clinoid Suprasellar area	Endoscopic endonasal Transsphenoidal Subfrontal Frontotemporal transsylvian Pterional transsylvian FTOZ Anterior interhemispheric
Frontal suprasinusal	Interhemispheric	Olfactory groove Suprasellar area Anterior third of the falx and SSS	Endoscopic endonasal Transsphenoidal Subfrontal transbasal Pterional transsylvian FTOZ Anterior interhemispheric
Coronaric suture (midline)	Interhemispheric	Middle third of the falx and SSS Third ventricle (anterior aspect)	Anterior interhemispheric Pterional trans-lamina terminalis Anterior transcallosal Anterior transcortical
Retrocoronaric (midline)	Interhemispheric	Middle third of the falx and SSS Third ventricle (posterior aspect)	Posterior interhemispheric Posterior transcallosal Posterior transcortical
Lambdoid suture (midline)	Interhemispheric	Posterior third of the falx and SSS Third ventricle (posterior aspect)	Posterior interhemispheric Posterior transcallosal Posterior transcortical
Inion	Supra-cerebellar infratentorial Suboccipital supratentorial	Superior tentorial surface Inferior tentorial surface Pineal region	Occipital transtentorial Supracerebellar infratentorial
Pterion	Presylvian	Sphenoid wing Sphenotemporal fossa Parasellar area	Frontotemporal transsylvian Pterional transsylvian FTOZ
Asterion	Cerebellopontine cistern	CPA angle Petroclival region	Retrosigmoid
Clivus	Transoral route	Clival region Paraclival region Magnum foramen	Retrosigmoid Far lateral Midline suboccipital
Kocher point	NA (intraparenchymal)	Lateral ventricle Monro foramen Suprasellar area	Anterior transcallosal/ transcortical Posterior transcallosal/ transcortical Superior parietal lobule FTOZ Frontotemporal trans sylvian Pterional transsylvian
Convexity	NA (intraparenchymal)	Cerebral convexity Intra-axial	Vault craniotomy

Abbreviations: CPA, cerebellopontine angle; FTOZ, frontotemporal orbitozygomatic; NA, not applicable; SSS, superior sagittal sinus.

volume, but once injected in the cadaver head it was only mildly effective in displacing stiff formalin-fixed cadaveric brain. Further, the requirement for MRI or CT imaging to ascertain the location and extent of the tumor lesion may be prohibitive in many neurosurgical laboratories.

Faster and More Effective Routes

A rigid K-wire (5 mm in width and 20 cm in length) was inserted into a Foley catheter through a single burr hole into the intracranial compartment under fluoroscopic guidance. Real-time skull X-rays guided the surgeon to precisely access the target area. We codified a map of burr holes and injection corridors used to place tumor in desired intracranial sites, reported in ►**Table 2** (►**Fig. 1**). The K-wire under C-arm guidance was a reliable method of minimally invasively reaching a highly precise target, using simple anatomical corridors that would not disrupt subsequent skull base surgical anatomy. Anatomical routes used to perform the injection were the interhemispheric fissure, the cerebellopontine cistern, the subfrontal, presylvian, suboccipital supratentorial, and the supracerebellar infratentorial corridors. The transoral route was used to inject the SRSDP into the

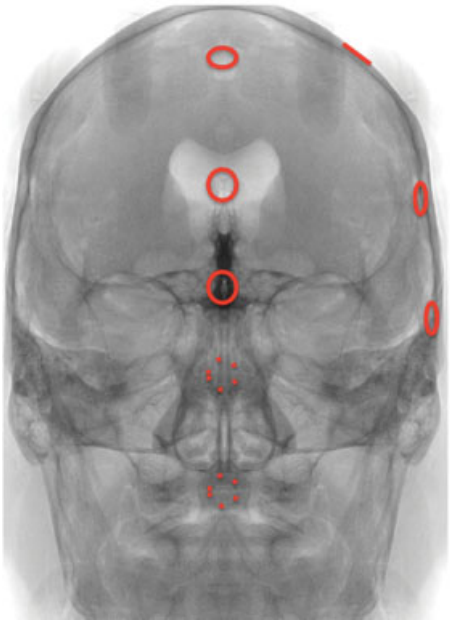

Fig. 1 Map of burr holes.

posterior cranial fossa (►**Fig. 2**). A transparenchymal injection route was preferred for lesions of centrally located lesions, such as those of the foramen of Monro, third and lateral ventricles, and suprasellar region. In these cases the injection device was inserted intraparenchymally through a burr hole placed at the Kocher point.

Injecting Bigger Lesions, Displacing the Brain to Create Mass Effect

Although the surgeons and residents who assessed our original injectable tumor model (ITM) provided positive feedback about their experience removing the lesions, one of the improvements desired was the ability to create mass effect.[1] In response, a simple and inexpensive device such as a Foley catheter served this purpose brilliantly. Once the target area was accessed with the K-wire on X-ray, the catheter balloon was minimally inflated with contrast agent under radiologic vision to confirm correct positioning. The Foley was then completely inflated and left in place for several minutes to displace anatomical structures and to create mass effect. In the meantime, SRSDP was prepared in a cup. As the polymerization reaction occurred, the catheter was deflated, and a minimal amount of the substance was injected through the needle, first in a liquid phase to enable subarachnoid spread. As SRSDP consistency began to change, the substance was completely injected under fluoroscopic vision into the target area, filling the void left by the deflated Foley catheter balloon (►**Fig. 3**).

To simulate intraparenchymal lesions, a smaller K-wire (2 mm width and 20 cm in length) was used. The needle was inserted into the brain parenchyma and the polymer injected with a high-pressure injection system, which enabled the substance to dissect white matter fibers, mimicking the growing pattern of a glial tumor. For cases of intraparenchymal lesions such as brain metastases with not only an infiltrative but also an expanding behavior, a single-lumen Fogarty catheter was additionally inflated to create the tumor bulk (►**Fig. 4**).

Image Processing

Once injected, the cadaveric heads were CT scanned with volumetric tools. A ray-tracing algorithm was used to render three-dimensional (3D) images of the specimens (►**Fig. 5**). Images were exported to the Neuronavigation system software (Brainlab) to plan the intraoperative neuronavigation. In case of lesions, presenting tight relationships with major vascular vessels, imaging of the cerebrovascular tree as described by Zhao and colleagues were also acquired.[3] The polymer matrix is visible on CT scan as a highly contrast-enhanced substance with a density easily distinguishable from bone and contrast-injected vascular vessels enabling preoperative planning. A postoperative CT scan can also be performed to assess the extent of surgical resection (►**Fig. 4C**).

Surgical Technique

Once injected with SRSDP, cadaveric specimens were fixed in a Mayfield three-point fixation head holder and placed in surgical position, in line with the approach to be performed. The operation performed was in accordance with tumor location and extension. Microsurgical techniques were conducted using a Zeiss OPM 1 FC (Carl Zeiss) and a rigid endoscope, 4 mm in diameter and 18 cm in length, with 0-, 30- and 45-degree lenses. A Midas Rex drill was used for bone drilling. A retrosigmoid approach was performed for tumors of the CPA; a cranio-orbitozygomatic-pterional-frontotemporal approach was used for tumors in the sellar and parasellar

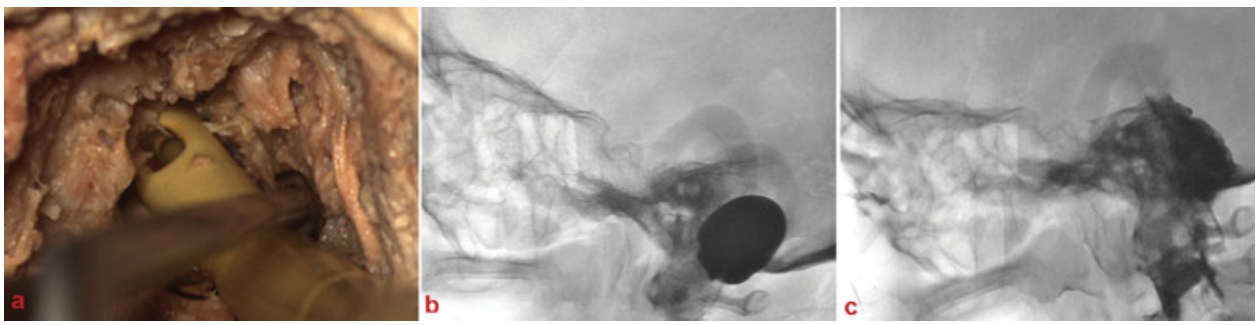

Fig. 2 Injection technique. (A) Transoral insertion of a Foley catheter into the posterior cranial fossa. (B) Floated catheter tip in the clival region. (C) Clival region after polymer injection.

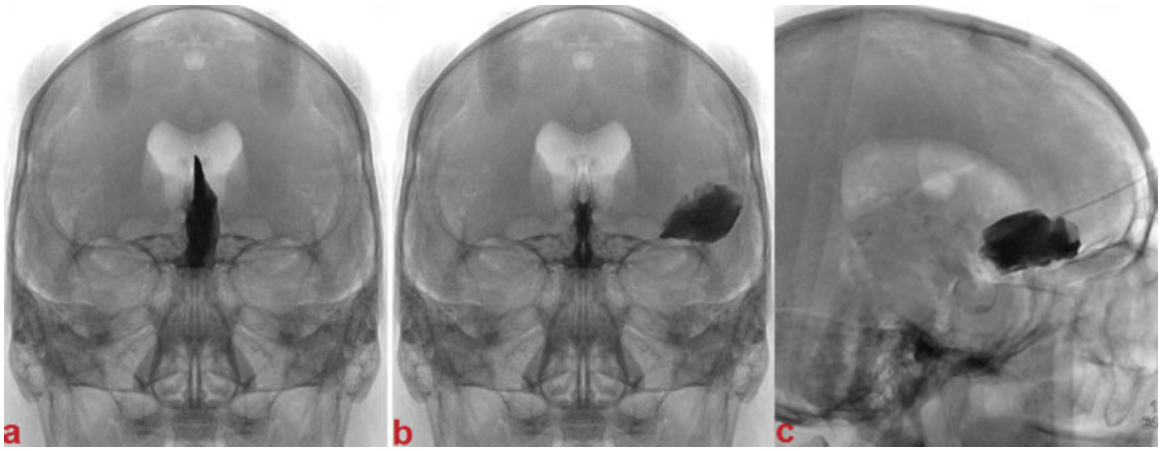

Fig. 3 Image processing. Appearance of X-rays after polymer injection. (A) Left anterior falx meningioma. (B) Left sphenoid wing meningioma. (C) Olfactory groove meningioma.

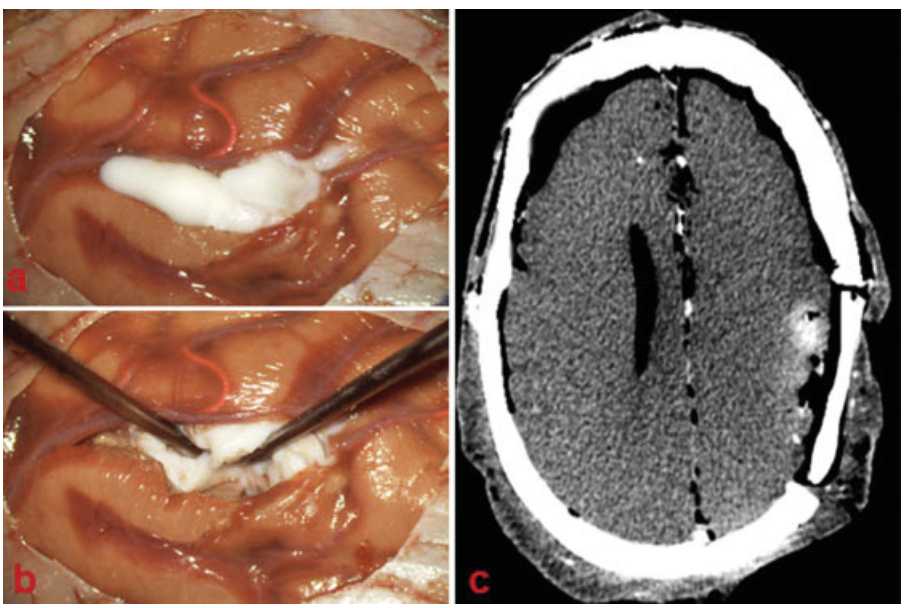

Fig. 4 Intraparenchymal lesion. (A) Polymer injected in the left parietal cortex. (B) Tumor dissection. (C) Postoperative computed tomography showing incomplete tumor resection.

areas (►**Fig. 6**), a far-lateral approach and midline suboccipital approach for those placed in the foramen magnum, and a supracerebellar infratentorial or suboccipital supratentorial approach for those placed on the inferior and superior tentorial surfaces, respectively. Ventricular lesions were accessed via anterior and posterior transcallosal/ transcortical approaches, and a superior parietal lobule approach. Subfrontal and sellar/ suprasellar lesions were resected either via a purely transnasal transsphenoidal endoscopic or a transbasal subfrontal approach (►**Videos 1** and **2**). Intra-axial lesions and convexity extra-axial tumors were accessed through a simple vault craniotomy, tailored with neuronavigation.

Video 1

Sellar and suprasellar tumor. Inserted via a frontal burr hole and resected via the endoscopic endonasal transsphenoidal approach.

Online content including video sequences viewable at: www.thieme-connect.com/products/ejournals/html/10.1055/s-0034-1368148.

Video 2

Anterior cranial fossa skull base tumor. Inserted via a frontal burr hole and resected via the expanded endonasal transsphenoidal transplanum approach.
Online content including video sequences viewable at: www.thieme-connect.com/products/ejournals/html/10.1055/s-0034-1368148.

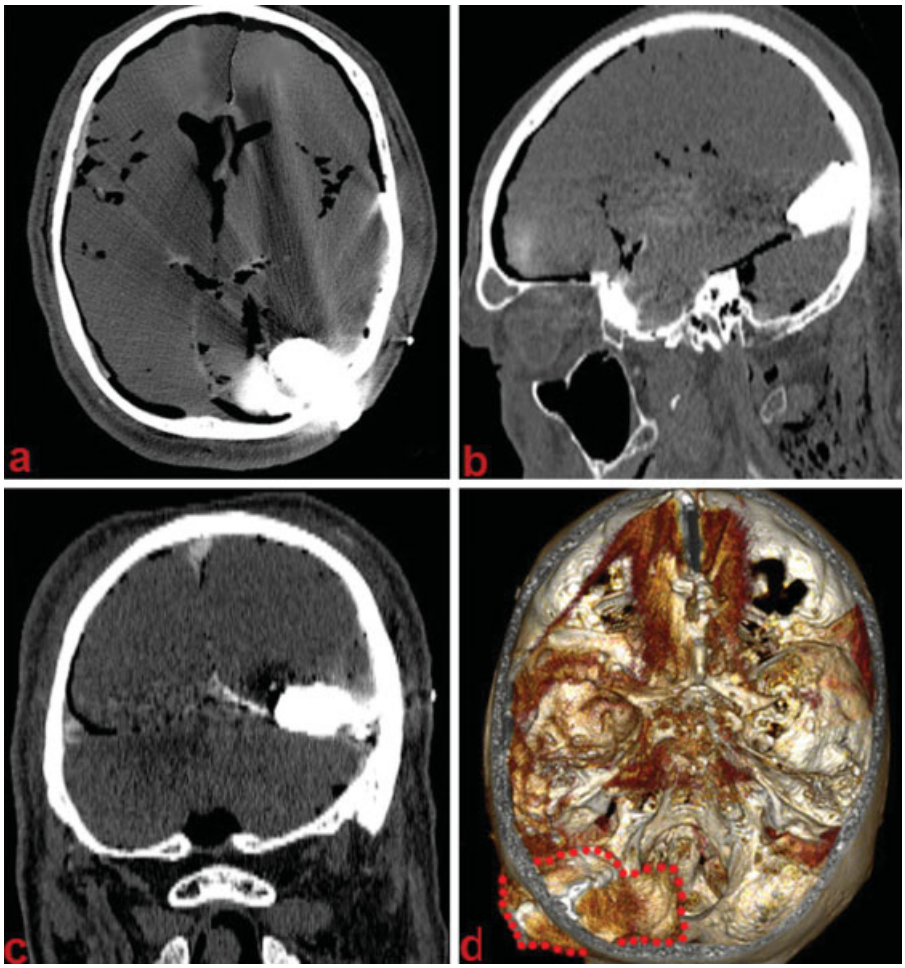

Fig. 5 Image processing. Computed tomography appearance after polymer injection. (A–C) Axial, sagittal, and coronal contrast-enhanced images of a large tentorial lesion. (D) Three-dimensional reconstruction algorithm (red dots highlight lesion margins).

Results

The ITM with SRSDP and cSRSDP simulated the difficulties and challenges of the surgical dissection around anatomical structures distorted by neoplastic masses. Residents and faculty surgeons evaluated the model in two different neurosurgical departments. Comparing SRSDP with SRS, we found that the modified polymer provided significantly better radiologic visibility. Contrast enhancement and proper radiologic density of SRSDP permitted an easy distinction from cranial bone and injected vessels, including also allowing for appreciation of the vessels encased within a lesion. The 3D reconstruction with volumetric acquisition of the images for neuronavigation allowed for precise preoperative planning and selection of an appropriate surgical approach.

Varying concentrations of the polymer allowed modification of the physical characteristics of SRSDP including deformability, viscosity, adhesiveness, subarachnoid spread potential, gumminess, friability, and stringing capacity. The previously mentioned chemical and physical characteristics imparted a proportional difficulty in microsurgical dissection technique and neoplastic tissue resectability. Piecemeal resection of the polymer became challenging for polymer concentrations $<$ 1:5. Dissection of tumor off surrounding neurovascular structures became technically demanding for polymer concentrations $<$ 1:7. Tumor relationships to adjacent neurovascular structures ranged from partial to complete encasement of vessels and nerves. In one case, high-pressure injection of the tumor on the upper tentorial surface caused transverse sinus fissuring and further sinus invasion by the tumor. Following injection of a CPA tumor, the tumor in its liquid phase extended into the internal auditory canal before solidifying, mimicking a vestibular schwannoma. In the case of intraparenchymal lesions, by injecting the polymer with a concentration of 1:3, the liquid phase spreads into the white matter dissecting the fibers and maintains a consistency that allows the tumor to be sucked, as in low-grade glioma surgery. The addition of fluorescein to the compound mimics fluorescein-guided resection.

The development of a minimally invasive, radiologic-controlled injection system, as just described, allowed for targeting precisely the injection site in any case. The only potential problem with the polymer injection involved the possibility of spilling material beyond the targeted area, if a quantity of polymer greater than what one intended was injected (i.e., 10 mL more than the initially intended quantity). In these cases we noticed a subarachnoid spread to a bigger area that did not affect the surgical experience but needed to be

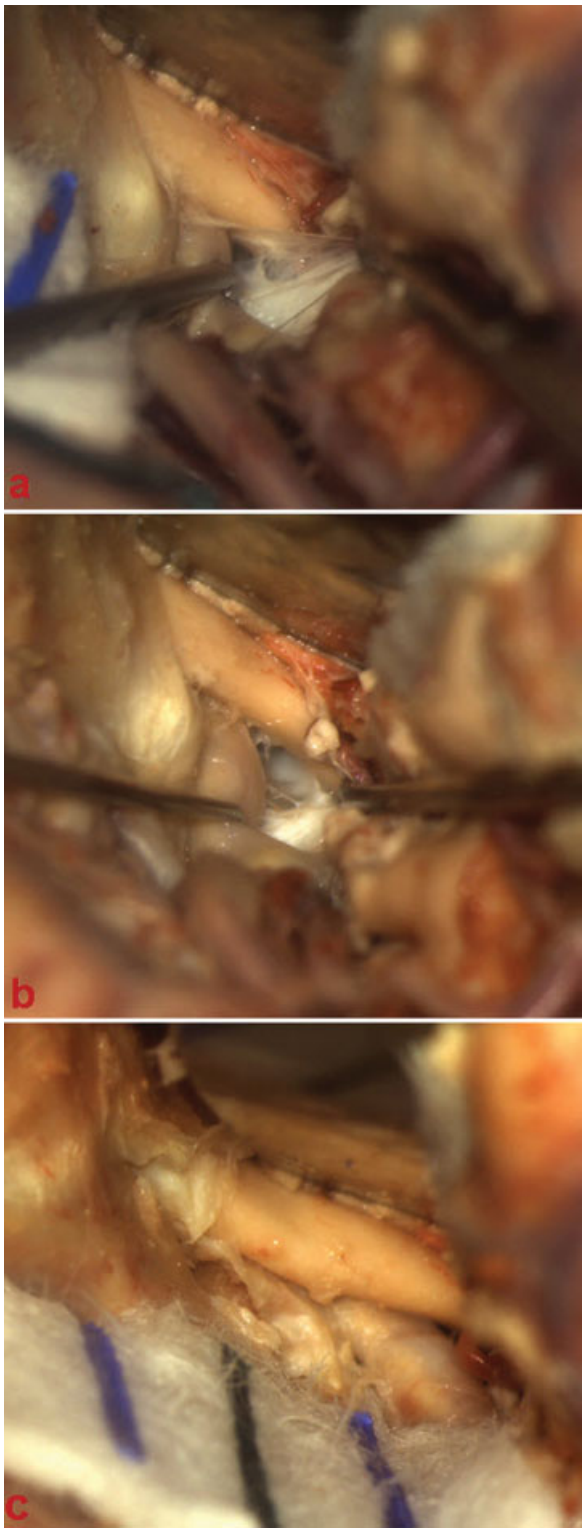

Fig. 6 Microscopic view. (A, B) Tumor dissection through the optic-carotid window. (C) Tumor extension into the optic canal after opening the optic sheet.

acknowledged when placing a second tumor afterward in a different location.

Time needed for tumor injection was significantly shorter when compared with the injection techniques of our previous ITM.[1] The process was easily reproducible and did not require particular surgical aptitude. Balloon catheter inflation simulated tumor bulk, distorting normal cadaveric anatomy into pathologic. Intraoperative views after gross total resection of the lesions demonstrated anatomical integrity of nerves and vessels, distorted by mass effect. Neurovascular displacement was particularly evident in the postoperative CT scan with the hypodensity of the resection cavity highlighted against the permanent enhancement of vascular structures.

Discussion

Since Harvey Cushing's apprenticeship under the supervision of Drs. William Halsted and William Osler, young neurosurgeons have trained under the tutelage of senior surgeons. Training in neurologic surgery is one of the most competitive and demanding specializations in medicine. It therefore demands careful planning in both the scientific and clinical neurosurgical arenas to produce physicians who can be technically sound and scientifically competitive.

In planning the formation of a European fellowship training program focused on neuro-oncology, the extreme difficulty of taking tumors out of the brain and the spine was recognized, but there was no solution proposed as to how to acquire the necessary skills.[4] In particular, in defining the objectives of such a long training program (1.5–2 years), it was proposed that the neurosurgeon (fellow) must demonstrate knowledge and skills in the application of all applicable innovative techniques and as surgeon responsible needs to manage 50 supra- and/or infratentorial tumors, 20 spinal tumors, and 30 computer-guided biopsy diagnostic procedures. It is unclear what being the surgeon responsible for these cases really means, and there is no mention to what set of skills will be transferred to the trainee.

The recent introduction of regulations limiting working hours for neurosurgical trainees carries the risk of compromising the amount of microneurosurgical training achieved during the period of residency and/or fellowship. This becomes more relevant when facing pathologic entities that are of higher complexity and/or lesions that are not encountered on a routine weekly basis such as tumors involving the cranial base. This anatomy is significantly altered in the presence of pathologic processes. In the absence of adequate surgical exposure to the pathologic state, an alternative option of a more continuous source of tactile and visual experience that simulates the real-life state is needed, which is still in its infancy in the field of neurosurgery.

Recently, increasing attention has been placed on the development of training models to improve both the microsurgical skills and anatomical knowledge of neurosurgical trainees. Microneurosurgical techniques and anatomical knowledge require extensive laboratory training before mastering these skills. There are diverse training models based on synthetic materials, anesthetized animals, animal cadavers, or human cadavers.[1,5–13] Human cadaver models are anatomically the most realistic with a main disadvantage of lack of hemodynamic factors. The first human cadaveric circulation model was described by Garret[8] followed by Aboud et al[6] who

created the dynamic pulsating cerebral model. Although many of these models are excellent, most have focused on performing surgical approaches in the setting of normal surgical anatomy. Very few of the currently available models expose the trainee to the anatomy distorted by a space-occupying lesion. The familiarity of the neurosurgical trainee with pathologic anatomy becomes more essential in the face of complex deep-seated skull base lesions.

Some of the greatest living neurosurgeons gave these issues consideration and tried to come up with reasonable models to solve this problem. Krisht et al, in particular, have developed a tumor model and is to date the only other model available to trainees to refine their surgical skills to extirpate these malignancies.[10] In their introduction they state, "the recent limitations of working hours for neurosurgical trainees carry the risk of decreasing the amount of microsurgical experience. In the absence of enough surgical exposure to some pathological states, an alternative option of a more continuous source of tactile and visual experience that simulates the real-life state is needed. To help with this problem, we established a cavernous sinus tumor model in the canine." This is a powerful statement. We so need to get trained on taking tumors out of these difficult locations that we are forced to put real tumors in canines to exercise our skills.

In an attempt to advance surgical training, we have discussed the features of an improved and simplified training model for skull base neurosurgery where a polymer is injected into a cadaver head to resemble a skull base tumor. The model has variable property characteristics allowing it to mimic a range of common brain tumors. The preparation procedure has been extremely simplified compared with the first application of the tumor model not requiring complicated approaches to the skull base, as described earlier, to apply a lesion under direct vision in the skull base leaving possible surgical corridors intact and available for the approach.

Conclusions

Many models have been proposed to improve training and surgical skills, and many have been used to teach the normal anatomy to both residents and young specialists. But to the best of our knowledge, almost none of them simulated tumor surgery, especially in cases of skull base tumors. Although knowledge of normal anatomy is the cornerstone of tumor surgery, one of the major difficulties for trainees when operating in real cases is how to deal with pathologic distorted anatomy. Another challenge is presented by the delicate microsurgical skills required for dissecting a tumor from the surrounding neural and vascular structures, which can be technically demanding and require a steep learning curve. We have addressed these two major hurdles of training by proposing this injectable tumor model. The physical characteristics of the polymer such as the presence of a dissection plane between tumor and the brain, as well as its consistency that is not "suckable" yet still able to be cut and dissected via microsurgical techniques, makes it closely resemble a true meningioma. The liquid phase of the tumor enables it to spread easily during insertion, even into distant, hidden, and difficult-to-access areas. For example, following injection of a CPA tumor, we found the tumor to extend into the internal auditory canal as in the case of real vestibular schwannoma, making the excision even more challenging and similar to live surgery. There is always a potential for modification and improvement of this model over time, and we hope that by exposing as many colleagues as possible to it we will be able to modify it to their needs.

References

1 Gragnaniello C, Nader R, van Doormaal T, et al. Skull base tumor model. J Neurosurg 2010;113(5):1106–1111
2 Sanan A, Abdel Aziz KM, Janjua RM, van Loveren HR, Keller JT. Colored silicone injection for use in neurosurgical dissections: anatomic technical note. Neurosurgery 1999;45(5):1267–1271, discussion 1271–1274
3 Zhao JC, Chen C, Rosenblatt SS, et al. Imaging the cerebrovascular tree in the cadaveric head for planning surgical strategy. Neurosurgery 2002;51(5):1222–1227; discussion 1227–1228
4 Cunha e Sá M. Additional competence training charter in neurosurgical oncology. Acta Neurochir (Wien) 2010;152(6):1095–1098
5 Abe M, Tabuchi K, Goto M, Uchino A. Model-based surgical planning and simulation of cranial base surgery. Neurol Med Chir (Tokyo) 1998;38(11):746–750; discussion 750–751
6 Aboud E, Al-Mefty O, Yaşargil MG. New laboratory model for neurosurgical training that simulates live surgery. J Neurosurg 2002;97(6):1367–1372
7 Buis DR, Buis CR, Feller RE, Mandl ES, Peerdeman SM. A basic model for practice of intracranial microsurgery. Surg Neurol 2009; 71(2):254–256
8 Garrett HE Jr. A human cadaveric circulation model. J Vasc Surg 2001;33(5):1128–1130
9 Hicdonmez T, Hamamcioglu MK, Parsak T, Cukur Z, Cobanoglu S. A laboratory training model for interhemispheric-transcallosal approach to the lateral ventricle. Neurosurg Rev 2006;29(2): 159–162
10 Krisht AF, Yoo K, Arnautovic KI, Al-Mefty O. Cavernous sinus tumor model in the canine: a simulation model for cavernous sinus tumor surgery. Neurosurgery 2005;56(6):1361–1365; discussion 1365–1366
11 Lannon DA, Atkins JA, Butler PE. Non-vital, prosthetic, and virtual reality models of microsurgical training. Microsurgery 2001; 21(8):389–393
12 Olabe J, Olabe J, Sancho V. Human cadaver brain infusion model for neurosurgical training. Surg Neurol 2009;72(6):700–702
13 Takeuchi M, Hayashi N, Hamada H, Matsumura N, Nishijo H, Endo S. A new training method to improve deep microsurgical skills using a mannequin head. Microsurgery 2008;28(3):168–170